EXAFS Studies of Nanocrystals of $Zn_{1-x}Mn_xO$: A Dilute Magnetic Semiconductor Oxide System

S. Chattopadhyay[1,2], S.D. Kelly[3], T. Shibata[1,2], R. Viswanatha[4], M. Balasubramanian[5], S. Stoupin[1], C.U. Segre[1], D.D. Sarma[4]

[1]Physics Division, BCPS Department, Illinois Institute of Technology, Chicago, IL 60616, USA; [2]Materials Research Collaborative Access Team (MRCAT) Argonne, IL 60439, USA; [3]Biosciences Division, Argonne National Laboratory, Argonne, Illinois 60439, USA; [4]Solid State and Structural Chemistry Unit, Indian Institute of Science, Bangalore 560012, India; [5]Advanced Photon Source, Argonne National Laboratory, Argonne, IL 60439, USA.

Abstract. Zn edge and Mn edge EXAFS studies have been performed on bulk and nanocrystals (4.7 nm) of the dilute magnetic semiconductor $Zn_{1-x}Mn_xO$, with x varying from 0.05 to 0.5. Preliminary analysis and linear combination fitting shows that Mn replaces Zn in the bulk sample, whereas in the nanocrystal samples, with different amounts of Mn, only a very small percentage of the Mn atoms replace Zn. The majority of the Mn atoms remain on the surface of the nanocrystallites in the form of Mn oxides.

Keywords: EXAFS, DMS, ZnO, nanocrystals, nanoparticles.
PACS: 61.46.Df

INTRODUCTION

Diluted magnetic semiconductors (DMSs) have attracted a great deal of attention in the last few years as enabling materials in the emerging field of spintronics [1]. DMSs are semiconductor solid solutions, with a small percentage of the cations replaced by magnetic ions such as Mn, Fe, etc. These materials exhibit properties dissimilar to those of the host compounds. The utilization of the charge of the electrons in the semiconductor host lattice and the spin of the electrons of the magnetic dopants can help in the fabrication of multifunctional devices with unique and novel properties [2]. Magnetically doped nanocrystals in dilute limits are a unique class of system that integrates both the semiconductor confinement effects like the optical properties arising out of finite size effects and magnetic properties arising out of the DMS nature of the system. The properties of the nanocrystal DMS and particularly oxide DMS, have remained largely unexplored. The unusual properties of these DMSs are strongly dependent on the local coordination, environment, bond length, bond angle, valence and the site symmetry of the magnetic ion as well as the host lattice. Hence, EXAFS is ideally suited for the study of these systems. We have performed Mn edge and Zn edge EXAFS measurements of bulk and nanocrystals (4.7 nm) of a doped semiconductor oxide ZnO-Mn, with Mn concentration varying from 0.5% to 5% in order to understand the local structure of the Mn dopant atoms in ZnO.

EXPERIMENTAL

Mn doped ZnO nanocrystals have been prepared by a novel wet chemical technique starting with Mn-acetate and Zn-acetate [3]. To obtain smaller sized particles of the order of 5 nm or less and uniform size distribution, the nanocrystals have been capped with polyvinylpyrollidone (PVP). Using this method nanocrystals with size varying from 3 to 6 nm, were prepared. The bulk samples were synthesized without the addition of PVP and by annealing the powders at 1200°C for 12 hours in air. The amount of Mn dopant was varied from 0.5% to 5%. The materials have been characterized by x-ray diffraction (XRD), atomic absorption spectroscopy (AAS), ultraviolet-visible absorption spectroscopy, transmission electron microscopy and electron paramagnetic resonance measurements. The XRD pattern of the nanocrystal samples shows the formation of wurtzite nanocrystals with similar lattice parameters as in the bulk. The size of the nanocrystals used in this study was determined from the XRD measurements to be 4.7 nm using the Scherrer formula.

CP882, *X-ray Absorption Fine Structure—XAFS13*
edited by B. Hedman and P. Pianetta

The Mn K-edge and Zn K-edge EXAFS measurements were performed at the MRCAT 10-ID beamline [4] and CMC-CAT 9-BM beamline respectively at the Advanced Photon Source, Argonne National Laboratory. Zn edge samples were spread on tape. Several layers were stacked so that the thickness x of the samples corresponded to $\Delta\mu x = 0.5$, where $\Delta\mu$ is the edge step of the absorption coefficient at the Zn K-edge energy. Mn edge measurements were made in fluorescence mode and the powder samples were mounted in plexiglass sample holders (1.5 mm diameter and 0.5 mm thick) for measurement. The Si(111) double crystal monochromator was scanned continuously so that the data was collected in quick EXAFS mode. The undulator parameters (taper and gap) were optimized to obtain a large photon flux with nearly constant intensity within the scanned energy range of 6,300 to 7,400 eV for the Mn edge.

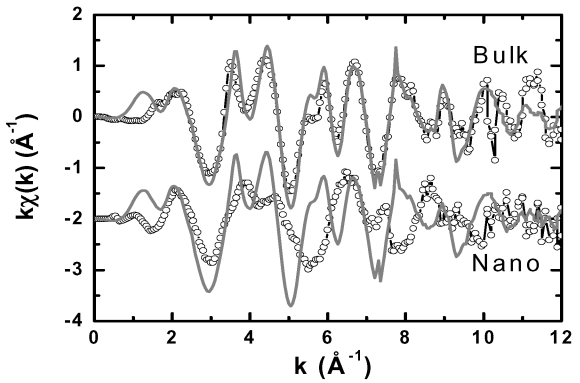

FIGURE 1. Comparison of Mn (symbol) and Zn (line) edge EXAFS spectra for the bulk (top) and nanocrystallite (bottom) samples with 1% Mn.

A Rh harmonic rejection mirror was used to eliminate x-rays of higher harmonic energies. Gases in the ion chambers were adjusted depending on the edge energy. The size of the incident x-ray beam on the sample was 1 mm^2. For the transmission measurements at the Zn edge (CMC-CAT), data were collected over the scanned energy range of 9,460 - 10,650 eV with a step size of 0.4 eV and a dwell time of 1.0 second. For each sample, 10 scans were taken and then averaged. For Mn edge measurements (MRCAT), the samples were found to degrade in the undulator beam when exposed for more than 8-10 minutes. Hence, quick scans were made with 0.3 eV step size; dwell time was 0.05 sec. Nine different locations were selected in each sample and 3 EXAFS scans were taken at each point. A total of 27 scans were summed for each of the nanocrystal samples.

The data was processed using the FEFFIT package [5]. Background subtraction and data merging was done with Athena [6]. Theoretical models were constructed with the program FEFF7 [7] and the crystallographic atomic positions of ZnO. The S_0^2 value for the Zn edge was set to 0.89 ± 0.06 as determined from a ZnO standard, and for the Mn edge it was set to 0.84 ± 0.06 as determined from a Mn_2O_3 standard.

RESULTS AND DISCUSSION

Figure 1 shows comparison of Mn (1%) and Zn edge EXAFS spectra for the bulk and the nanocrystal samples. The Mn edge data from bulk samples resemble the Zn spectra of the same sample. This suggests that Mn atoms replace Zn atoms in the bulk sample. The spectra from the 1% Mn nanocrystal (size = 4.7 nm) sample is very different from the Zn edge spectra for the same sample, which indicates that majority of Mn is not replacing Zn in the nanocrystal samples.

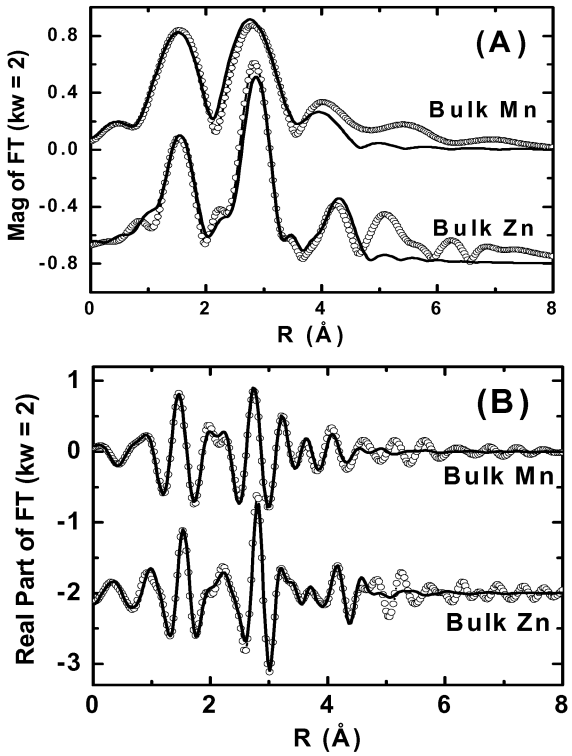

FIGURE 2. Bulk Mn-edge and Zn-edge EXAFS data (symbols) and model (line) based on substitution of Mn for Zn in the ZnO structure. Figures (A) and (B) are the magnitude and real part, respectively of the Fourier transform (FT) of the data and model fit. The fit range is from 0 to 4.5 Å. The data range is from 4.0 to 8.0 Å^{-1} for the Mn spectra and 4.5 to 12.0 Å^{-1} for the Zn spectra.

The bulk Mn and Zn spectra sets were simultaneously fit in R-space with k-weighting of 1, 2 and 3 in the Fourier transform of the data and the model was simultaneously optimized to both data sets

with exactly the same parameters to verify that Mn replaces Zn within the bulk sample. As shown in figure 2, the model can describe the features of both data sets. The magnitude and real part of the Fourier transform of the fit for a k-weight of 2 is shown in Figure 2. Fit values for the energy shift E_0 are -2.3 ± 1.5 eV and 0.1 ± 1.4 eV for the Mn and Zn data, respectively. The σ^2 values and distances are the same for the Mn edge and Zn edge spectra. The fit values for the lattice constants a and c are 3.19 ± 0.02Å and 5.34 ± 0.02Å respectively. In this model two σ^2 for oxygen shells and three σ^2 for Zn shells were determined by the fit to the measured spectra. These values are listed in Table 1. The same model was applied to the Zn and Mn spectra from the nanocrystal sample, but was not successful in reproducing both spectra (data not shown).

TABLE 1. EXAFS fitting results for co-refinement of Mn and Zn edge (represented as X) spectra for the bulk ZnO-Mn 1% sample.

Path	X-O_1	X-O_2	X-Zn_1	X-Zn_2	X-Zn_3
R (Å)	1.98 (0.01)	1.95 (0.01)	3.24 (0.01)	3.19 (0.02)	3.55 (0.02)
$\sigma^2(10^{-3}$ Å$^2)$	6(1)	4(1)	7(1)	16(4)	10(2)

From XANES analysis, the Mn absorption edge of the DMS nanocrystal samples lie between that of Mn^{2+} and Mn^{4+} standards. Hence, the Mn edge spectra of the nanocrystal samples were modeled with a linear combination of Mn oxide standards. The best fit was obtained with a combination of 1% Mn within bulk ZnO, MnO_2, Mn_3O_4 and Mn_2O_3. Figure 3 shows the linear combination fit of all four nanocrystal samples with different concentrations of Mn. The percentages of various oxide forms required for a best fit, are listed in Table 2. We observe that very few Mn atoms have replaced Zn in the nanocrystal samples, as shown by the small fraction (only a few percent) of the signal

TABLE 2. Fit results from linear combination fit of the Mn edge spectra of the various nanocrystal (4.7 nm) samples.

Standards	Sample ZnO-Mn (0.5%)	Sample ZnO-Mn (1.0 %)	Sample ZnO-Mn (2.3 %)	Sample ZnO-Mn (5.0 %)
bulk ZnO 1% Mn	2±2 %	3±2 %	0 %	2±2 %
MnO_2	14±3 %	29±3 %	19±2 %	19±2 %
Mn_3O_4	57± 1%	60±4 %	64±3%	57± 4 %
Mn_2O_3	28± 6%	16±5%	17±4%	23± 5 %

that is similar to the ZnO sample with 1% Mn. A majority of the Mn atoms exist in an environment similar to that of Mn in Mn_3O_4 and smaller quantities resemble Mn in Mn_2O_3 and MnO_2.

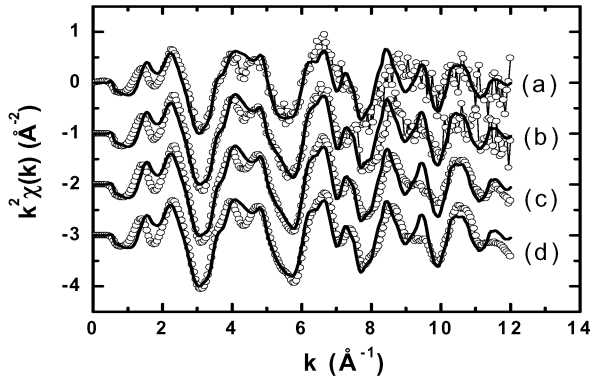

FIGURE 3. Linear combination data (symbols) and fit (solid line) of the 4.7 nm sized Mn doped samples: (a) 0.05% Mn, (b) 1% Mn, (c) 2.3% Mn and (d) 5% Mn.

CONCLUSION

Our preliminary studies of Mn and Zn edges of the DMS system $Zn_{1-x}Mn_xO$ (x varying from 0.05 to 0.5) indicate that in bulk DMS samples, the Mn atoms replace the Zn atoms. In nanocrystals (4.7 nm) of DMS, a very small percentage of the Mn atoms replace the Zn atoms. Majority of the Mn atoms are present on the surface of the nanocrystallites in the form of various oxides.

ACKNOWLEDGMENTS

The authors would like to thank Trudy Bolin of CMC-CAT for providing beamline support. MRCAT is funded by the MRCAT member institutions (http://mrcat.iit.edu). The APS is funded by the U. S. Department of Energy, Office of Basic Energy Sciences under Contract number W-31-109-Eng-38.

REFERENCES

1. I. Zutic, J. Fabian and S. Das Sarma, *Rev. Mod. Phys.* **76,** 323 (2004).
2. H. Ohno, *Science* **281**, 951 (1998).
3. R. Viswanatha, S. Sapra, S. Sen Gupta, B. Satpati, P.V. Satyam, B.N. Dev and D.D. Sarma *J. Phys. Chem. B* **108**, 6303 (2004).
4. C.U. Segre, et al. *Synchrotron Radiation Instr*: Eleventh U.S. Conference **CP521**, 419-422 (2000).
5. E.A. Stern, M. Newville, B. Ravel, Y. Yacoby and D. Haskel, *Physica B* **208** & **209**, 117 (1995).
6. M. Newville, *J. Synchr. Radiation.* **8**, 322 (2001).
7. S.I. Zabinsky, J.J. Rehr, A. Andukinov, R.C. Albers and M.J. Eller *Phys. Rev. B* **52**, 2995 (1995).